Feeling the force: how pollen tubes deal with obstacles

Burri, Jan T ; Vogler, Hannes ; Läubli, Nino F ; Hu, Chengzhi ; Grossniklaus, Ueli ; Nelson, Bradley J

Abstract: Physical forces are involved in the regulation of plant development and morphogenesis by translating mechanical stress into the modification of physiological processes, which, in turn, can affect cellular growth. Pollen tubes respond rapidly to external stimuli and provide an ideal system to study the effect of mechanical cues at the single-cell level. Here, pollen tubes were exposed to mechanical stress while monitoring the reconfiguration of their growth and recording the generated forces in real-time. We combined a lab-on-a-chip device with a microelectromechanical systems (MEMS)-based capacitive force sensor to mimic and quantify the forces that are involved in pollen tube navigation upon confronting mechanical obstacles. Several stages of obstacle avoidance were identified, including force perception, growth adjustment and penetration. We have experimentally determined the perceptive force threshold, which is the force threshold at which the pollen tube reacts to an obstacle, for Lilium longiflorum and Arabidopsis thaliana. In addition, the method we developed provides a way to calculate turgor pressure based on force and optical data. Pollen tubes sense physical barriers and actively adjust their growth behavior to overcome them. Furthermore, our system offers an ideal platform to investigate intracellular activity during force perception and growth adaption in tip growing cells.

DOI: https://doi.org/10.1111/nph.15260

Feeling the force: how pollen tubes deal with obstacles

Jan T. Burri[1,*], Hannes Vogler[2,*], Nino F. Läubli[1], Chengzhi Hu[1], Ueli Grossniklaus[2,†],and Bradley J. Nelson[1,†]

burrija@ethz.ch, hannes.vogler@botinst.uzh.ch, laeublin@ethz.ch, huc@ethz.ch, grossnik@botinst.uzh.ch, bnelson@ethz.ch.

[1]Multi-Scale Robotics Lab, Department of Mechanical and Process Engineering, ETH Zürich, 8092 Zürich, Switzerland

[2]Department of Plant and Microbial Biology and Zürich-Basel Plant Science Center, University of Zürich, 8008 Zürich, Switzerland

[*]these authors contributed equally to this work

[†]Correspondence to: grossnik@botinst.uzh.ch, +41 44 634 82 40; bnelson@ethz.ch, +41 44 632 55 29

Word count: 3709 (main body), 893 (Introduction), 842 (Materials and Methods), 1340 (Results), 595 (Discussion), 39 (Acknowledgement)

Number of figures: 5 (all in color)

Number of supplementary videos: 2

Summary

- Physical forces are involved in the regulation of plant development and morphogenesis by translating mechanical stress into the modification of physiological processes, which, in turn, can affect cellular growth. Pollen tubes respond rapidly to external stimuli and provide an ideal system to study the effect of mechanical cues at the single-cell level. Here, pollen tubes were exposed to mechanical stress while monitoring the reconfiguration of their growth and recording the generated forces in real-time.
- We combined a lab-on-a-chip device with a microelectromechanical systems (MEMS)-based capacitive force sensor to mimic and quantify the forces that are involved in pollen tube navigation upon confronting mechanical obstacles. Several stages of obstacle avoidance were identified, including force perception, growth adjustment, and penetration.
- We have experimentally determined the perceptive force threshold, which is the force threshold at which the pollen tube reacts to an obstacle, for *Lilium longiflorum* and *Arabidopsis thaliana*. In addition, the method we developed provides a way to calculate turgor pressure based on force and optical data.
- Pollen tubes sense physical barriers and actively adjust their growth behavior to overcome them. Furthermore, our system offers an ideal platform to investigate intracellular activity during force perception and growth adaption in tip growing cells.

Keywords: cellular force microscopy, force perception, lab-on-a-chip, MEMS-based capacitive force sensor, penetrative forces, perceptive force, pollen tubes, single cell

Introduction

The integration of physical stress, growth, and development has attracted burgeoning attention in plant developmental biology. Plant cells are able to respond to external physical forces in several ways, for example by directing cell wall synthesis to the site of increased stress, or by modifying biochemical and biophysical processes to regulate cell expansion (Hamant *et al*., 2008; Heisler *et al*., 2010; Ellinger & Voigt, 2014; Kesten *et al*., 2017). The ability to perceive mechanical forces is fundamental to all plant cells (Darwin & Darwin, 1881; Jaffe, 1973; Jaffe & Forbes, 1993; Braam, 2004; Chehab *et al.*, 2009). Until now, numerous studies have shown the effect of external mechanical forces on the growth patterns of plant organs (thigmomorphogenesis) with respect to cytoskeletal organization, cell wall integrity,

biosynthesis, cellular anisotropy in expansion, and patterns of phytohormone responses (Lintilhac & Vesecky, 1981; Haley *et al.*, 1995; Yahraus *et al.*, 1995; Wymer *et al.*, 1996; Legué *et al.*, 1997; Lynch & Lintilhac, 1997; Hamant *et al.*, 2008; Haswell *et al.*, 2008; Monshausen & Haswell, 2013).

Pollen, comprising a vegetative cell that encloses the two sperm cells, forms a cellular protrusion called the pollen tube (PT), which forms upon pollen hydration and germination. The PT grows through stylar and ovarian tissues to reach the ovules, where it bursts and releases the two sperm cells to effect double fertilization (Borg *et al.*, 2009). The advancing apex of the elongating PT, driven by turgor pressure, generates forces large enough to penetrate through these tissues. During their growth, PTs need to perceive external mechanical obstacles and exert sufficient penetrative forces. Meanwhile, PTs need to reconfigure their growth behavior to withstand externally applied compressive stress. The PT with its fast growth rate and rapid response to external stimuli offers a perfect model system to investigate the impact of mechanical cues at the single-cell level (Chebli & Geitmann, 2007). The molecular mechanisms underlying the accurate navigation of the PT towards the ovule, by perceiving and responding to guidance cues, have been thoroughly investigated over the last decade. Numerous chemotropic factors have been identified, such as sugars, calcium, nitric oxide, lipids, adhesins, and secreted peptide signals serving as guidance cues (Hülskamp *et al.*, 1995; Ray *et al.*, 1997; Wolters-Arts *et al.*, 1998; Mollet, 2000; Higashiyama *et al.*, 2003; Prado *et al.*, 2004; Sanati Nezhad *et al.*, 2014; Higashiyama & Yang, 2017; Qu *et al.*, 2015).

Until now, the vast majority of research on PT guidance has focused on the mediation of directional growth by biochemical factors. However, a major hurdle for the PT on its way to the ovule is the physical interaction with the surrounding tissues. The growing interest on the influence of mechanical forces acting as cues for cellular behavior and thereby regulating growth and morphogenesis, has triggered the demand for new techniques to study the effect of mechanical stimuli at the single-cell level. With the advances in microelectromechanical systems (MEMS) and microfluidics, various lab-on-a-chip (LOC) devices have been fabricated for the high-throughput analysis of PTs and their interactions with biochemical and mechanical cues (Horade *et al.*, 2013; Agudelo *et al.*, 2013; Sanati Nezhad *et al.*, 2014; Shamsudhin *et al.*, 2016; Yanagisawa *et al.*, 2017; Hu *et al.*, 2017a,b). Despite the insights offered by these LOC devices, they still lack the ability to directly measure the variation of cytomechanical properties or the forces exerted on the PTs. Force values have to be extracted using modeling methods, such as finite element method (FEM)-based models, which has been done for example to predict the penetrative force of *Camellia japonica* PTs (Sanati Nezhad *et al.*, 2013). Values

derived from models are usually approximations and strongly depend on the accuracy of the model and its input parameters, and validation can be difficult. Most models can only partially incorporate the complex nature of cytomechanical phenomena, and the trade-off between accuracy and available computation power makes it difficult to model dynamic processes. Therefore, an immediate force readout is crucial to correlate the applied forces and the triggered intracellular effects, such as the adaption of growth, changes in material properties, or intracellular signaling cascades that are set in motion. Until now, direct measurements of forces exerted by tip-growing cells have only been performed on fungal hyphae, where the measurement was conducted with a silicon bridge strain gauge (Johns *et al*., 1999; Money, 2007). However, the low-resolution force of 1 µN, the manual calibration, and the inadaptability of the orientation of the sensor with respect to the hyphae, have hindered the broad use of this technique.

Merging the flexibility of microfluidic design with the direct and immediate force readout of a MEMS-based capacitive force sensor (Enikov & Nelson, 2000; Sun & Nelson, 2007) opens up new ways to investigate the effect of forces and stress on the growth and physiology of tip-growing cells. In this study, an *in vitro* environment was designed by combining microfluidics and MEMS force-sensing to mimic the PT's journey from stigma to ovary while simultaneously assessing the arising forces and observe the changes in the PT's growth behavior. The perceptive force threshold, defined as the force at which the PTs react to a mechanical barrier by changing their growth direction, has been determined in two different species, *Lilium longiflorum* (lily) and *Arabidopsis thaliana*. Furthermore, the penetrative force of the PTs, when they squeeze through a microgap, was quantified and correlated to geometrical factors and turgor pressure.

Materials and Methods

System Integration, Control and Data Acquisition

To simulate the natural environment of PTs *in vitro*, we designed a system that forces the PTs to grow against a mechanical barrier or to squeeze through narrow gaps, while we simultaneously recorded the generated forces in real-time. The system combines a LOC for high-throughput pollen germination and guided parallelized PT growth, adapted from previous work by Shamsudhin et al. (2016), with a cellular force microscope (CFM) (Vogler *et al*., 2013; Felekis *et al*., 2011; Felekis *et al*., 2014; Felekis *et al*., 2015; Burri *et al.*, 2016), equipped with a commercially available lateral force sensor (FT-S1000-LAT, FemtoTools AG) (Fig. 1a).

The LOC was fabricated by soft lithography using polydimethylsiloxane (PDMS) with an elastomer base to curing agent mass ratio of 10:1 (Young's modulus E = 2.6 MPa (Wang *et al.*, 2004)) and provides a reservoir, in which the pollen grains germinate. After germination, the PTs grow into parallel microchannels with square cross-sectional areas of 25×25 µm (height×width) for lily (Fig. 1b) and 7×9 µm for *Arabidopsis*.

The capacitive MEMS sensor offers a high-resolution force-sensing plate of 50×50 µm (Fig. 1c), which was placed at the end of the microchannels and acted as an obstacle with integrated force readout (Fig. 1d). Within the force range of ±1000 µN, the force signal is captured using an analog input module (NI 9215, National Instruments). In our experiments, force values were read out at 50 kHz. Data output was reduced to 50 Hz by averaging 1'000 consecutive readouts, giving a standard deviation of the force signal of 0.18 µN. For precise three-dimensional control, the force sensor was mounted on an aluminum arm on a piezoelectric xyz positioner with a closed loop resolution of 4 nm (SLC-2475-S, SmarAct GmBH). The positioner allowed the distance between the force plate and the microchannel to be adjusted to form a narrow gap, mimicking the small cavities in the apoplast between cells along the PT's path to the ovule.

The experiments were recorded with a 40x objective lens (LUCPlanFL N 40x, Olympus) mounted on an inverted microscope (IX71, Olympus) using a CCD camera (Orca-D2, Hamamatsu). High-resolution imaging enabled us to capture the real-time response of PTs when interacting with mechanical obstacles and to correlate them with the direct force measurements. An xy stage (M-687.UO, Physik Instrumente (PI) GmbH & Co.) integrated into the microscope, was actuated by a piezomotor controller with a sensor resolution of 0.1 µm (C-867.262, PI GmbH & Co.), and used to position the sample in the field of view. Data acquisition and the control of the xy stage and the xyz positioner were implemented in LabVIEW™ (National Instruments (NI)).

Data Analysis

Data analysis was performed in MATLAB (MathWorks). To objectively determine the perceptive force threshold, i.e., when the force values reach a plateau, data were filtered (second order Savitzky-Golay-filter) and a polynomial fit was applied to the force curve. The perceptive force threshold was given as the local maximum ($f'(x) = 0, f''(x) < 0$) prior to the plateau (Fig. 2b, Fig. 3b). If the plateau never reached a completely flat level due to a subsequent force increase (e.g. Fig. 4b), the perceptive force threshold was assigned to the local point with the smallest slope ($f''(x) = 0, f'''(x) > 0$).

Pollen Tube Preparation

Anthers of *Lilium longiflorum* were placed in Eppendorf tubes, and stored at −80 °C. To germinate the PTs, pollen grains were rehydrated in humid chambers for 30 min at room temperature, after which they were mixed with PT growth medium (PTGM) and filled into the LOC device. PTs were grown in solidified growth medium. Lily PTGM is: 160 µM H_3BO_3, 130 µM $Ca(NO_3)_2$, 1 mM KNO_3, 5 mM MES and 10 % sucrose at a pH of 5.5. To solidify the medium, we added 1 % ultra-low-gelling agarose (A2576, Sigma-Aldrich). Solid PTGM was stored at 4 °C, re-melted at 63 °C, and equilibrated at 23 °C before mixing with rehydrated pollen grains and loading into the LOC device. To solidify the agarose within the microchannels, the LOC was cooled at 4 °C for 4 min. Excess agarose in front of the channels was removed with a wooden toothpick. This is important to avoid interference of agarose with the force sensor. The reason for using solidified growth medium was to simulate the mechanical resistance of the transmitting tissue in plants. As a positive side effect, the pollen in the agarose solution showed a more stable growth pattern over a longer time periods compared to those growing in liquid PTGM. The glass slides in front of the LOC where the PTs emerge were treated with poly-*L*-lysine (P4832-50ML, Sigma-Aldrich), forming a monolayer to improve the adhesion of the PTs to the glass slide.

Flowers of *Arabidopsis thaliana*, accession Col-0, were collected and incubated for 30 min at 22 °C in a moisture chamber. PTs were grown in solidified PTGM (1.6 mM H_3BO_3, 5 mM $CaCl_2$, 5 mM KCl, 1 mM $MgSO_4$, and 10 % sucrose at a pH of 7.5). The solidification of agarose and LOC loading followed the same procedure as described for lily PTs.

Results

Pollen tubes perceive the force exerted by obstacles and react with a change in growth behavior

The ability to sense mechanical stress or forces is crucial for cells to adapt their growth and shape according to changing environmental conditions. PTs with their fast growth rates and their invasive behavior must rapidly adapt their growth according to external mechanical stimuli. The interaction of the growing PTs with physical barriers and the forces generated reveal a tactile perception in lily PTs.

In our experiments, the PTs were guided along parallel microchannels to achieve unidirectional growth and to ensure a perpendicular contact with the force-sensing plate placed at a distance larger than the PT

diameter from the channel exit. This gap allowed the PT to change growth direction without restrictions from the LOC channels. Using the force-sensing plate as a mechanical obstacle offered real-time force readout, which allowed us to measure the force parallel to the growth direction of the PTs (Supporting Information Video S1). After the initial contact of the PTs with the sensor plate, a sharp force increase was observed (Fig. 2b i) while the apical region was symmetrically compressed (Fig. 2a i-ii). This passive deformation was observed up to a force with a mean value of 9.6 ± 1.6 µN in lily (n = 30, Fig. 2b ii and 2c). After that point, the force remained constant, indicating that the PT stopped growing (Fig. 2b ii-iii). After a short lag phase (typically a few seconds), the PT resumed growth, which was accompanied by a change in growth direction, visible as a small bulge perpendicular to the original growth axis (Fig. 2a iii). At the last stage, the force remained at a constant level (Fig. 2b iv) while the PT tip grew along the force plate (Fig. 2a iv).

The observed growth arrest indicates that lily PTs can sense physical obstacles and react to this external mechanical stimulus by adjusting their growth direction in order to avoid obstacles. Since this critical force threshold marks the moment that the PT perceives and responds to the force, we refer to it as the perceptive force threshold (Fig. 2c).

Force perception is not species-specific

Lily PTs have a comparably large diameter and are easy to manipulate. Their disadvantage is that genetic tools, such as mutant or transgenic lines, do not exist, making it difficult to examine the physiological and molecular basis of force perception. However, all these tools are available in *Arabidopsis*, another model species in plant biology. Therefore, we repeated the experiments using *Arabidopsis* PTs to test whether the observed force sensing behavior was general or species-specific. The observed change in growth (Fig. 3a) together with the force pattern (Fig. 3b) revealed that *Arabidopsis* PTs behave analogously to lily PTs when confronted with a physical barrier. In the case of *Arabidopsis*, however, a perceptive force threshold of 3.0 ± 0.6 µN was measured (n = 10, Fig. 3c), which is considerably lower than the one measured for lily PTs. The subsequent change in growth direction was more prominent in *Arabidopsis*, leading to a sharp, almost perpendicular bending after interacting with the force-sensing plate (Fig. 3a iv). The results of the comparison between lily and *Arabidopsis* suggest that force sensing in PTs may be a conserved mechanism, which is common to mono- and dicotyledonous plant species.

Invasive Growth: Penetration follows Perception

Apart from sensing and reacting to external mechanical obstacles, PTs can exert forces on their environment. This is crucial for invading cells in surrounding tissue (i.e. stigmatic papillar cells) or squeezing between transmitting tract cells, and eventually delivering the sperm cells to the ovules. In our experiment, the force sensing plate was placed close to the exit of the microchannels forming a narrow gap (smaller than the PT diameter), through which the PT could penetrate (Fig. 4a). The gap simulated the path of the PT through the apoplast growing within or between cells, and the penetration of the ovule through the micropyle and the filiform apparatus.

Lily PTs showed a clear sequence of behaviors when squeezing through the artificially created barrier (Supporting Information Video S2). This sequence consisted of five stages corresponding to initial contact, perception, adaptation, penetration, and emergence. The first two stages (Fig. 4a i-ii) were equivalent to the interactions discussed in the previous section. After recognizing the mechanical barrier, the PTs adjusted their growth direction and, when confronted with a narrow opening, anchored themselves with a small protrusion within the gap (Fig. 4a iii). If the apex was already close to the small opening this phase was very short, but occasionally the PT first bent into several directions until it located a suitable interstice. Once detected, the PT squeezed into the slim lacuna and slightly widened it by the forces it generated (Fig. 4a iv). At last, the PT emerged from the channel and continued to grow while returning to its original shape (Fig. 4a v).

The measured force was correlated with the individual phases during the interaction. In the experiment, we observed that different PTs showed similar force patterns (Fig. 4b) and a representative schematic force curve is illustrated in figure 4c, where the five penetration stages are highlighted. The force sharply increased after the PT contacted the force plate (Fig. 4c i). After perceiving the mechanical obstacle, the force stopped increasing and formed a small plateau in the force curve (Fig. 4c ii). When the PT adapted its growth direction and sought a way to overcome the barrier, the forces varied around a constant value (Fig. 4c iii). With the chasm found, the slope of the force curve increased while the apex entered the small gap. Once the whole apex had completely entered the constriction, an almost linear increase of the force with time was observed (Fig. 4c iv). When the PT emerged from the gap, the force remained constant (Fig. 4c v).

The penetrative force, generated at the flank of the PT when squeezing through the gap, was obtained by subtracting the force values prior to the penetration (i.e. the perceptive force threshold) from the force measured after emerging, and was in the range of several tens of μN up to 85 μN, with a mean

value of 29 ±18 µN (n = 21, Fig. 5a). The large variation of these values arose due to dependencies of the measured maximal forces on geometrical factors of the gap and the PT itself.

The penetrative force (F_p) is given by the contact area A multiplied with the turgor pressure P at the time when the PTs emerge from the gap. Since the cell wall that is in contact with the force plate runs parallel to it, its tension T does not contribute to the measured forces (Fig. 5b). The width and length of the gap, as well as the diameter of the PT after emerging can be extracted from the optical recordings. The contact area of the PT with the sensor can be estimated using these values. Assuming that the circumference of the PT remains unaffected by exiting the gap, we can equate the perimeter U of the apex after emerging with the one during the penetration,

$$U = d_{tip}\pi = w_{gap}\pi + 2w_{contact} \quad (1)$$

The contact area A is then determined by

$$A_{contact} = l_{gap} \cdot w_{contact} = l_{gap}\frac{(d_{tip}-w_{gap})\pi}{2} \quad (2)$$

where d_{tip} is the PT tip diameter, w_{gap} the gap width, l_{gap} the gap length, and $w_{contact}$ the contact width between the PT and sensor plate (Fig. 5b).

The ratio between penetrative force $F_{penetrative}$ and contact area A yields the turgor pressure P (Fig. 5c) of the PT when it grows out from the channel according to

$$P = \frac{F_{penetrative}}{A_{contact}} \quad (3)$$

A turgor pressure of (0.19 ± 0.09) MPa was derived from our measurements, which is consistent with the reported values of 0.1 MPa to 0.4 MPa for lily (Benkert *et al*., 1997).

The penetrative force depends mainly on the geometry of the gap. An upper bound of these forces is only given when the gap is too small for the PT to invade or if the gap is too long for the PT to penetrate. The force is created by the deformation of the PT and the turgor pressure.

Discussion

On their way to the ovule, PTs have to deal with obstacles by either avoiding or invading them. This implies a perception mechanism, which allows them to sense and react to the forces that are involved.

Although, several studies estimated the forces that are exerted by tip-growing cells (i.e., Money, 2007; Sanati Nezhad *et al*., 2013), technological limitations did not allow correlations between small force changes and subtle alterations in growth behavior. Therefore, we developed a system capable of measuring forces in real-time at high resolution while simultaneously monitoring the growing PTs.

The experimental system combines a LOC device and a MEMS force sensor to create physical obstacles with an integrated force readout. The growth of tip growing single cells, e.g. PTs, is directionally guided onto a defined obstacle with adjustable gap sizes. This allows the study of interactions between tip growing cells and mechanical barriers, thereby assessing the influence of external mechanical stimuli onto their perceptive behavior and response. The capability to directly measure the forces arising between the cell and the sensor plate can immediately correlate force changes with the corresponding growth behavior and adaption.

Our system is designed to study how PTs perceive mechanical cues and adapt their growth behavior to navigate around obstacles and squeeze through narrow openings. Their reaction to external mechanical stress as well as the forces they exert on their environment were monitored. A perceptive force threshold of 9.6 µN in lily and 3.0 µN in *Arabidopsis* PTs was observed. After the perceptive force threshold was reached, the PTs sensed the obstacle and adjusted their apical growth direction in order to avoid it. This suggests the presence of mechanosensitive receptors, such as stretch-activated ion channels, in the apical region as previously reported (Dutta and Robinson, 2004). However, we cannot exclude the involvement of mechanosensitive receptors in more distal regions (Hamilton *et al*., 2015) through mechanical coupling to the force applied at the apex. PTs were able to penetrate through tiny gaps by first anchoring themselves with a small protrusion. The narrower and longer the gap the PT had to penetrate through, the larger the observed force. Penetrative forces of up to 85 µN were measured. An estimation of the contact area allowed us to calculate the pressure the PT exerted on the force plate, which corresponded to the turgor pressure of the PT at the moment when it emerged from the gap.

PT growth is guided by biochemical, electrical, and mechanical cues, but it is largely unknown how these cues are internally processed. To gain information about changes in the physiological properties induced by growth changes, it is necessary to observe intracellular processes at high spatial and temporal resolution. The design of the LOC facilitates microscopy by confining the PTs to a single focal plane. Hence, intracellular activities can be investigated during the PT–force sensor interactions, for example by observing the effects of mechanical stress on physiological parameters using fluorescent

biosensor molecules. Therefore, our system will be instrumental in identifying new molecules and pathways that are involved in mechanotransduction. PTs facilitate penetration by secreting chemical factors to modify the mechanical resistance of the surrounding tissue, which suggests a coupling between mechanical cues and chemical secretion (Wu *et al*., 1996; Dearnaley and Daggard, 2001; Hiscock *et al.*, 2002). The system described here will be instrumental in exploring to what extent this mechanism is linked to the perception of external forces and stress. Although our experiments were focused on PTs, the configuration can be adapted to characterize other tip-growing cells, such as root hairs, moss protonemata, or fungal hyphae.

Acknowledgements

This work was financed through ETH Zürich and the University of Zürich, and a Research and Technology Development (RTD) project (MecanX - Understanding Physics of Plant Growth) of SystemsX.ch, the Swiss Initiative in Systems Biology (to U.G. and B.J.N.).

Author contributions

U.G. and B.J.N. initiated and supervised the project, and raised funding. J.T.B. and H.V. conceptualized the project and designed, conducted, and analyzed the experiments, N.F.L. designed and fabricated the LOC device. C.H. provided know-how and suggestions. J.T.B. and H.V. wrote the manuscript. All authors reviewed and commented on the manuscript.

References

Agudelo CG, Sanati Nezhad A, Ghanbari M, Naghavi M, Packirisamy M, Geitmann A. 2013. TipChip: a modular, MEMS-based platform for experimentation and phenotyping of tip-growing cells. *The Plant Journal* **73**: 1057–1068.

Benkert R, Obermeyer G, Bentrup F-W. 1997. The turgor pressure of growing lily pollen tubes. *Protoplasma* **198**: 1–8.

Borg M, Brownfield L, Twell D. 2009. Male gametophyte development: a molecular perspective. *Journal of Experimental Botany* **60**: 1465–1478.

Braam J. 2004. In touch: plant responses to mechanical stimuli. *New Phytologist* **165**: 373-389.

Burri JT, Hu C, Shamsudhin N, Wang X, Vogler H, Grossniklaus U, Nelson BJ. 2016. Dual-axis cellular force microscope for mechanical characterization of living plant cells. *2016 IEEE International Conference on Automation Science and Engineering (CASE 2016)*, Fort Worth, USA: 942-947.

Chebli Y, Geitmann A. 2007. Mechanical principles governing pollen tube growth. *Functional Plant Science and Biotechnology* **1**: 232–245.

Chehab EW, Eich E, Braam J. 2009. Thigmomorphogenesis: a complex plant response to mechano-stimulation. *Journal of Experimental Botany* **60**: 43–56.

Darwin C, Darwin F. 1881. *The power of movement in plants*. New York, USA: D. Appleton and Company.

Dutta R, Robinson KR. 2004. Identification and characterization of stretch-activated ion channels in pollen protoplasts. *Plant Physiology* **135**: 1398-1406.

Dearnaley JDW, Daggard GA 2001. Expression of a polygalacturonase enzyme in germinating pollen of Brassica napus. *Sexual Plant Reproduction* **13**: 265–271.

Ellinger D, Voigt C. 2014. Callose biosynthesis in *Arabidopsis* with a focus on pathogen response: what we have learned within the last decade. *Annals of Botany* **114**: 1349–1358.

Enikov ET, Nelson BJ. 2000. Three-dimensional microfabrication for a multi-degree-of-freedom capacitive force sensor using fibre-chip coupling. *Journal of Micromechanics and Microengineering* **10**: 492–497.

Felekis D, Muntwyler S, Vogler H, Beyeler F, Grossniklaus U, Nelson BJ. 2011. Quantifying growth mechanics of living, growing plant cells in situ using microrobotics. *Micro & Nano Letters* **6**: 311-316.

Felekis D, Vogler H, Mecja G, Muntwyler S, Nestorova A, Huang T, Sakar MS, Grossniklaus U, Nelson BJ. 2015. Real-time automated characterization of 3D morphology and mechanics of developing plant cells. *The International Journal of Robotics Research* **34**: 1136–1146.

Felekis D, Vogler H, Mecja G, Muntwyler S, Sakar MS, Grossniklaus U, Nelson BJ. 2014. High-throughput analysis of the morphology and mechanics of tip growing cells using a microrobotic platform. *2014 IEEE/RSJ International Conference on Intelligent Robots and Systems (IROS 2014)*, Chicago, USA: 3955–3960.

Haley A, Russell AJ, Wood N, Allan AC, Knight M, Campbell AK, Trewavas AJ. 1995. Effects of mechanical signaling on plant cell cytosolic calcium. *Proceedings of the National Academy of Sciences of the United States of America* **92**: 4124–4128.

Hamant O, Heisler M, Jönsson H, Krupinski P, Uyttewaal M, Bokov P, Corson F, Sahlin P, Boudaoud A, Meyerowitz E, Couder Y, Traas J. 2008. Developmental patterning by mechanical signals in *Arabidopsis*. *Science* **322**: 1650–1655.

Hamilton ES, Schlegel AM, Haswell ES. 2015. United in diversity: mechanosensitive ion channels in plants. *Annual Review of Plant Biology* **66**: 113-137.

Haswell ES, Peyronnet R, Barbier-Brygoo H, Meyerowitz EM, Frachisse J-M. 2008. Two MscS homologs provide mechanosensitive channel activities in the *Arabidopsis* root. *Current Biology* **18**: 730–734.

Heisler M, Hamant O, Krupinski P, Uyttewaal M, Ohno C, Jönsson H, Traas J, Meyerowitz E. 2010. Alignment between PIN1 polarity and microtubule orientation in the shoot apical meristem reveals a tight coupling between morphogenesis and auxin transport. *PLoS Biology* **8**: e1000516.

Higashiyama T, Kuroiwa H, Kuroiwa T. 2003. Pollen-tube guidance: beacons from the female gametophyte. *Current Opinion in Plant Biology* **6**: 36–41.

Higashiyama T, Yang W-C. 2017. Gametophytic pollen tube guidance: attractant peptides, gametic controls, and receptors. *Plant Physiology* **173**: 112–121.

Hiscock S, Bown D, Gurr S, Dickinson H 2002. Serine esterases are required for pollen tube penetration of the stigma in *Brassica*. *Sexual Plant Reproduction* **15**: 65–74.

Horade M, Kanaoka MM, Kuzuya M, Higashiyama T, Kaji N. 2013. A microfluidic device for quantitative analysis of chemoattraction in plants. *RSC Advances* **3**: 22301-22307.

Hu C, Munglani G, Vogler H, Fabrice TN, Shamsudhin N, Wittel FK, Ringli C, Grossniklaus U, Herrmann HJ, Nelson BJ. 2017a. Characterization of size-dependent mechanical properties of tip-growing cells using a lab-on-chip device. *Lab on a Chip* **17**: 82–90.

Hu C, Vogler H, Aellen M, Shamsudhin N, Jang B, Burri JT, Läubli N, Grossniklaus U, Pané S, Nelson BJ. 2017b. High precision, localized proton gradients and fluxes generated by a microelectrode device induce differential growth behaviors of pollen tubes. *Lab on a Chip* **17**: 671–680.

Hülskamp M, Schneitz K, Pruitt R. 1995. Genetic evidence for a long-range activity that directs pollen tube guidance in *Arabidopsis*. *The Plant Cell* **7**: 57–64.

Jaffe MJ. 1973. Thigmomorphogenesis: the response of plant growth and development to mechanical stimulation. *Planta* **114**: 143–157.

Jaffe MJ, Forbes S. 1993. Thigmomorphogenesis: the effect of mechanical perturbation on plants. *Plant Growth Regulation* **12**: 313–324.

John S, Davis CM, Money NP. 1999. Pulses in turgor pressure and water potential: resolving the mechanics of hyphal growth. *Microbiological Research* **154**: 225–231.

Kesten C, Menna A, Sànchez-Rodrìguez C. 2017. Regulation of cellulose synthesis in response to stress. *Current Opinion in Plant Biology* **40**: 106– 113.

Legué V, Blancaflor E, Wymer C, Perbal G, Fantin D, Gilroy S. 1997. Cytoplasmic free Ca^{2+} in *Arabidopsis* roots changes in response to touch but not gravity. *Plant Physiology* **114**: 789–800.

Lintilhac PM, Vesecky TB. 1981. Mechanical stress and cell wall orientation in plants. II. The application of controlled directional stress to growing plants; with a discussion on the nature of the wound reaction. *American Journal of Botany* **68**: 1222–1230.

Lynch TM, Lintilhac PM. 1997. Mechanical signals in plant development: a new method for single cell studies. *Developmental Biology* **181**: 246–256.

Mollet JC, Park SY, Nothnagel EA, Lord, EM. 2000. A lily stylar pectin is necessary for pollen tube adhesion to an in vitro stylar matrix. *The Plant Cell* **12**: 1737–1749.

Money NP. 2007. Biomechanics of invasive hyphal growth. In: Howard RJ, Gow NAR., eds. *Biology of the fungal cell*. Heidelberg: Springer: 237–249.

Monshausen GB, Haswell ES. 2013. A force of nature: molecular mechanisms of mechanoperception in plants. *Journal of Experimental Botany* **64**: 4663–4680.

Prado AM, Porterfield DM, Feijó, JA. 2004. Nitric oxide is involved in growth regulation and re-orientation of pollen tubes. *Development* **131**: 2707–2714.

Qu LJ, Li L, Lan Z, Dresselhaus T. 2015. Peptide signaling during the pollen tube journey and double fertilization. *Journal of Experimental Botany* **66**: 5139–5150.

Ray SM, Park SS, Ray A. 1997. Pollen tube guidance by the female gametophyte. *Development* **124**: 2489–2498.

Sanati Nezhad A, Naghavi M, Packirisamy M, Bhat R, Geitmann A. 2013. Quantification of cellular penetrative forces using lab-on-a-chip technology and finite element modeling. *Proceedings of the National Academy of Sciences* **110**: 8093-8098.

Sanati Nezhad A, Packirisamy M, Geitmann A. 2014. Dynamic, high precision targeting of growth modulating agents is able to trigger pollen tube growth reorientation. *The Plant Journal* **80**: 185–195.

Shamsudhin N, Laeubli N, Atakan HB, Vogler H, Hu C, Haeberle W, Sebastian A, Grossniklaus U, Nelson BJ. 2016. Massively parallelized pollen tube guidance and mechanical measurements on a lab-on-a-chip platform. *PLoS ONE* **11**: e0168138.

Sun Y, Nelson BJ. 2007. MEMS capacitive force sensors for cellular and flight biomechanics. *Biomedical Materials* **2**: 16-22.

Vogler H, Draeger C, Weber A, Felekis D, Eichenberger C, Routier-Kierzkowska A-L, Boisson-Dernier A, Ringli C, Nelson BJ, Smith RS, Grossniklaus U. 2013. The pollen tube: a soft shell with a hard core. *The Plant Journal* **73**: 617–627.

Wang Z, Volinsky AA, Gallant ND. 2014. Crosslinking effect on polydimethylsiloxane elastic modulus measured by custom-built compression instrument. *Journal of Applied Polymer Science*, **131**: 41050.

Wolters-Arts M, Lush WM, Mariani C. 1998. Lipids are required for directional pollen-tube growth. *Nature* **392**: 818–821.

Wu Y, Qiu X, Du S, Erickson L 1996. PO149, a new member of pollen pectate lyase-like gene family from alfalfa. *Plant Molecular Biology* **32**: 1037–1042.

Wymer CL, Wymer SA, Cosgrove DJ, Cyr RJ. 1996. Plant cell growth responds to external forces and the response requires lntact microtubules. *Plant Physiology* **110**: 425–430.

Yahraus T, Chandra S, Legendre L, Low PS. 1995. Evidence for a mechanically induced oxidative burst. *Plant Physiology* **109**: 1259–1266.

Yanagisawa N, Sugimoto N, Arata H, Higashiyama T. 2017. Capability of tip-growing plant cells to penetrate into extremely narrow gaps. *Scientific Reports* **7**: 1403.

Figure legends

Fig 1. System configuration to simulate the natural environment of the pollen tube (PT) in vitro with integrated force readout. (a) The experimental system combines a lab-on-a-chip (LOC) device with a

microelectromechanical systems (MEMS)-based force sensor. (b) An optical image of a LOC loaded with pollen grains in the inner reservoir; the PTs grow in parallel in the same focal plane through the microchannels. (c) Capacitive force sensor measuring lateral forces at the force-sensing plate. (d) Schematic side-view of the experimental setup where the force-sensing plate is placed in front of the PTs emerging from the microchannels.

Fig 2. Force perception in lily pollen tubes (PT) when confronted with an obstacle measured by a microelectromechanical systems (MEMS) force sensor. (a) The PTs adjust their apical growth direction in response to external mechanical cues: (i) initial contact, (ii) passive deformation, (iii) adjustment of apical growth direction, and (iv) bending of the shank. (b) Forces generated between PT tip and force sensing plate during the interaction: (i) initial contact, (ii) perceptive force threshold, (iii-iv) stable force. (c) Descriptive statistics of the perceptive force threshold in lily PTs. Red line indicates the median, blue box indicates the 25^{th} and 75^{th} percentile and the whiskers extend to the most extreme data points not considered outliers.

Fig 3. Force perception in *Arabidopsis* pollen tubes (PTs). (a) Similar to the lily PTs, *Arabidopsis* PTs adjust their apical growth direction in response to external mechanical cues: (i) initial contact, (ii) passive deformation, (iii-iv) adjustment of apical growth direction. (b) Forces generated between the PT tip and the force plate during the interaction. (i) initial contact and (ii) perceptive force threshold. (c) Descriptive statistics of the perceptive force threshold in *Arabidopsis* PTs. Red line indicates the median, blue box indicates the 25^{th} and 75^{th} percentile, red cross indicates outliers and the whiskers extend to the most extreme data points not considered outliers.

Fig 4. Forces exerted by lily pollen tubes (PTs) growing through a small gap (a) Five different stages of the PT's interaction to sense and overcome a barrier by penetrating through a narrow gap: (i) initial contact, (ii) passive deformation, (iii) adjustment of growth direction and anchoring in the gap, (iv) gap penetration, (v) emerging from the gap. (b) Force curves of individual PTs when confronted with a mechanical barrier (force sensor) and subsequent squeezing through a narrow gap. All the tested PTs show a similar response when interacting with a mechanical obstacle. (c) A schematic force curve representing the akin force curves and highlighting the different stages.

Fig 5. Penetrative force measurements can be used to calculate turgor pressure during penetration. (a) Descriptive statistics of the penetrative force generated by lily pollen tubes (PTs). (b) Schematic representation of the generated force F during penetration in dependence of internal pressure P, cell wall tension T and the contact area $A_{contact}$ which is approximated by the following geometrical features: length of the gap l_{gap}, width of the gap w_{gap}, width of the contact area $w_{contact}$ and diameter of the PT tip d_{tip}. (c) Descriptive statistics of the ratio between the penetrative force and the contact area yields the turgor pressure of the PTs after they emerged. Boxplots: Red line indicates the median, blue box indicates the 25^{th} and 75^{th} percentile, red cross indicates outliers, and the whiskers extend to the most extreme data points not considered outliers.

Supporting Information

Video S1. Force perception of a lily pollen tube when confronted with an obstacle measured by a microelectromechanical systems (MEMS) force sensor.

Video S2. Forces exerted by a lily pollen tube growing through a small gap.

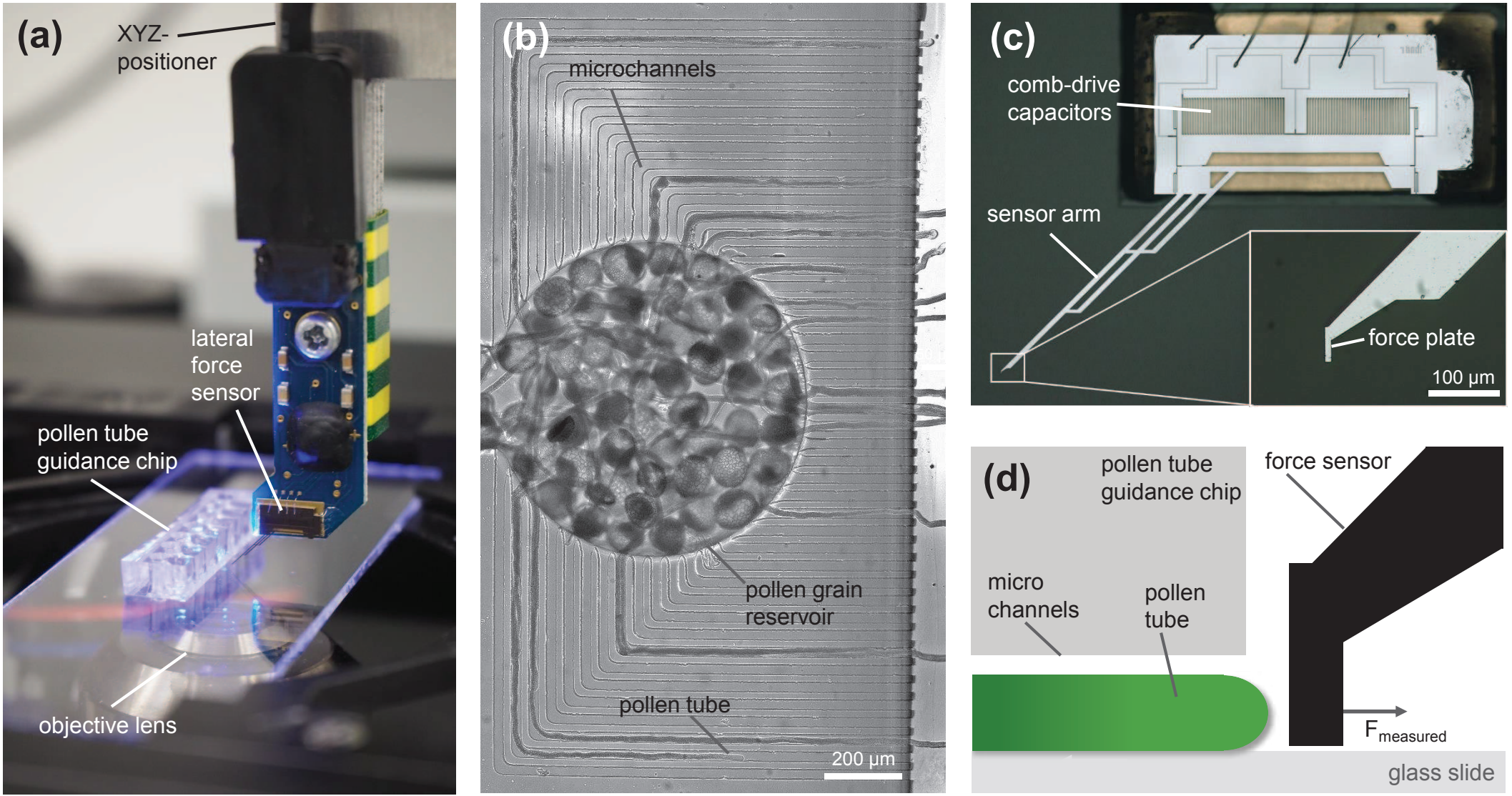
(a)
XYZ-
positioner
lateral
force
sensor
pollen tube
guidance chip
objective lens
(b)
microchannels
pollen grain
reservoir
pollen tube
200 µm
(c)
comb-drive
capacitors
sensor arm
force plate
100 µm
(d)
pollen tube
guidance chip
force sensor
micro
channels
pollen
tube
F measured
glass slide

Fig. 1

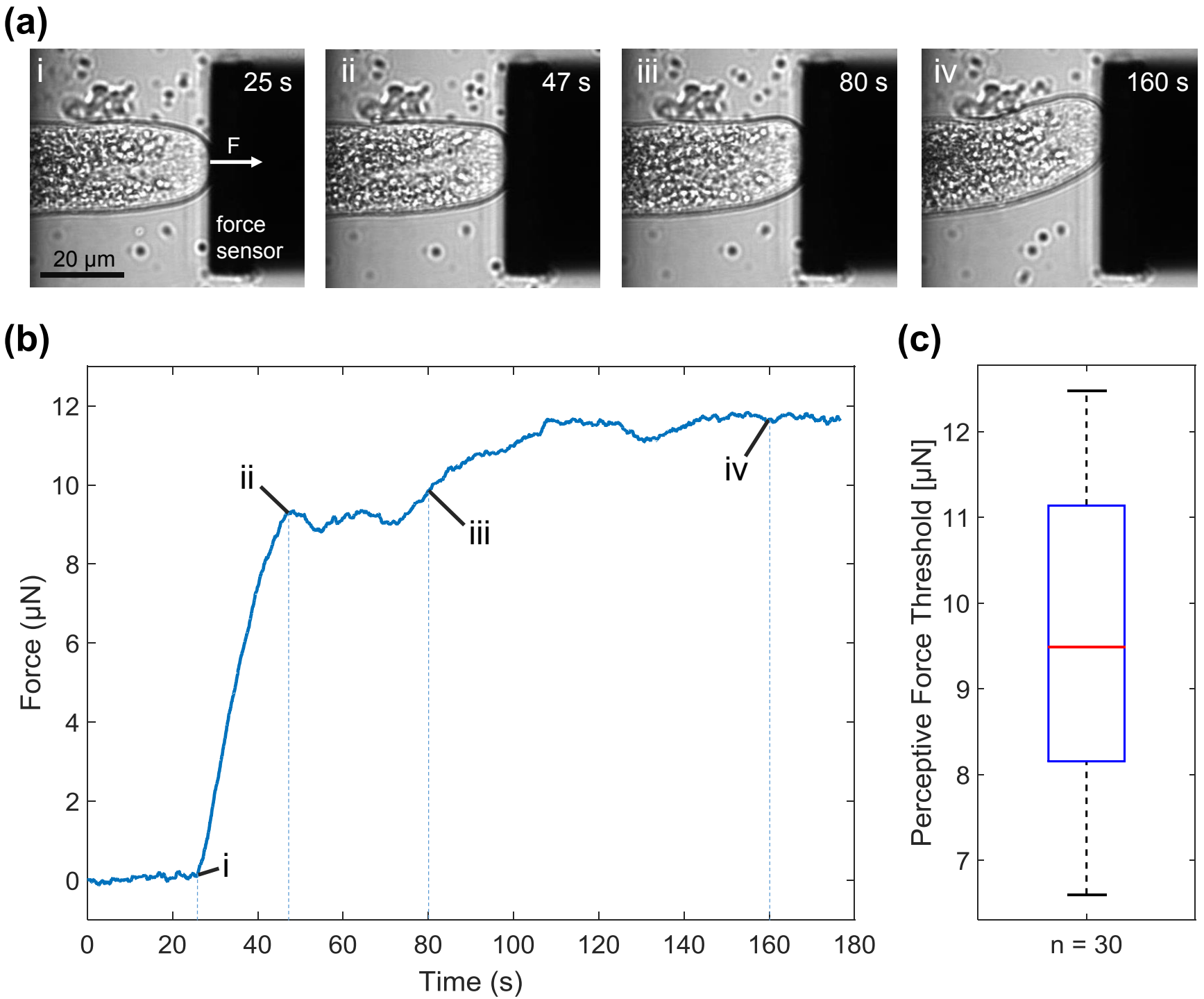
(a)
i
25 s
F
force
sensor
20 μm
ii
47 s
iii
80 s
iv
160 s
(b)
Force (μN)
Time (s)
i
ii
iii
iv
0
2
4
6
8
10
12
0
20
40
60
80
100
120
140
160
180
(c)
Perceptive Force Threshold [μN]
7
8
9
10
11
12
n = 30

Fig. 2

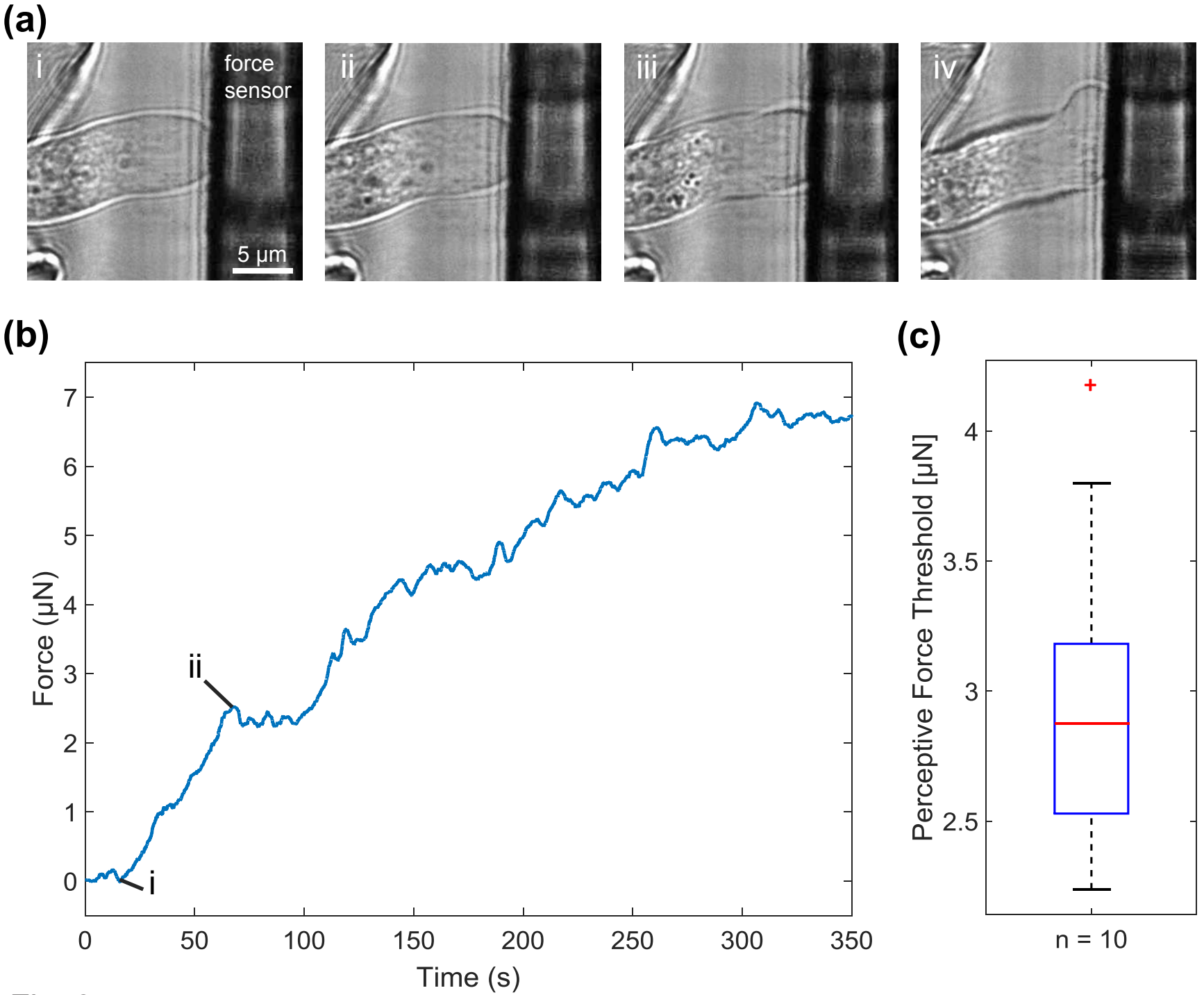
(a)
i
force sensor
5 µm
ii
iii
iv
(b)
Force (µN)
Time (s)
ii
i
0
1
2
3
4
5
6
7
0
50
100
150
200
250
300
350
(c)
Perceptive Force Threshold [µN]
2.5
3
3.5
4
n = 10

Fig. 3

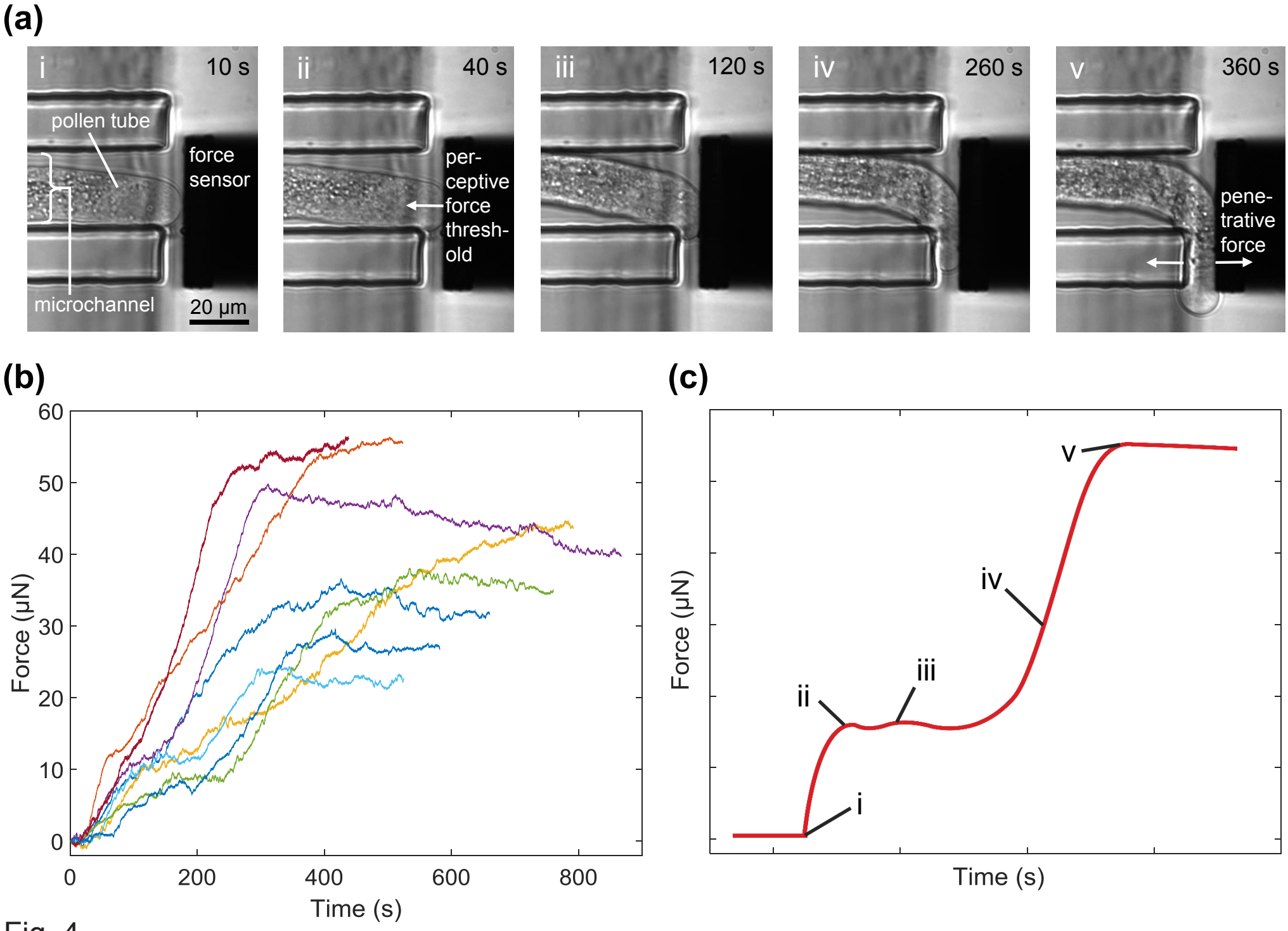
(a)
i
10 s
pollen tube
force sensor
microchannel
20 μm
ii
40 s
per-ceptive force thresh-old
iii
120 s
iv
260 s
v
360 s
pene-trative force
(b)
Force (μN)
Time (s)
0
10
20
30
40
50
60
0
200
400
600
800
(c)
Force (μN)
Time (s)
i
ii
iii
iv
v

Fig. 4

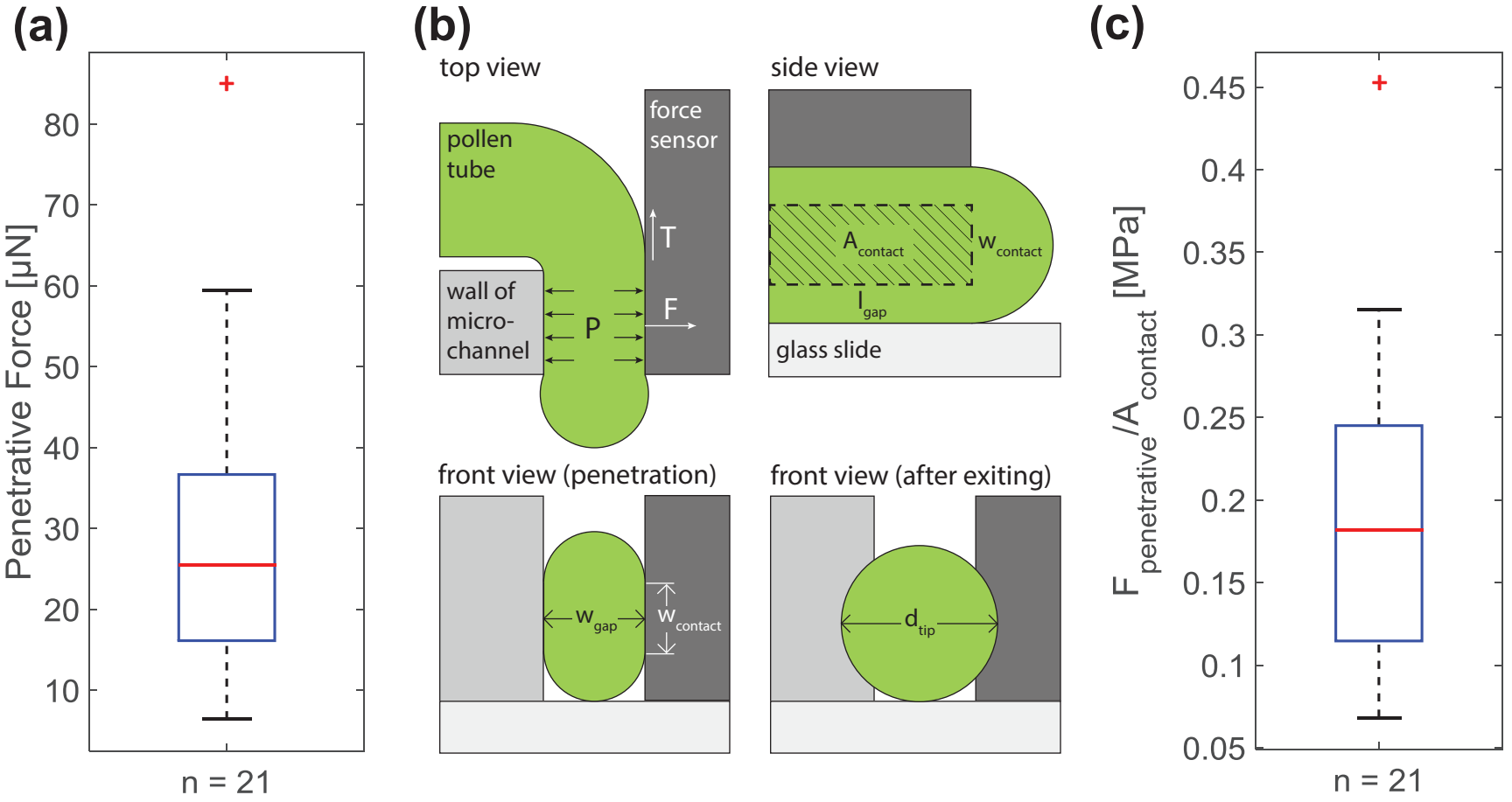
(a)
Penetrative Force [µN]
80
70
60
50
40
30
20
10
n = 21
(b)
top view
pollen tube
force sensor
T
wall of micro-channel
P
F
side view
A contact
w contact
l gap
glass slide
front view (penetration)
w gap
w contact
front view (after exiting)
d tip
(c)
F penetrative /A contact [MPa]
0.45
0.4
0.35
0.3
0.25
0.2
0.15
0.1
0.05
n = 21

Fig. 5